



Published in final edited form as:

*Mucosal Immunol.* 2014 September ; 7(5): 1221–1232. doi:10.1038/mi.2014.12.

## Neutrophil-derived JAML Inhibits Repair of Intestinal Epithelial Injury During Acute Inflammation

Dominique A. Weber<sup>1,\*</sup>, Ronen Sumagin<sup>1,\*</sup>, Ingrid C. McCall<sup>1</sup>, Giovanna Leoni<sup>1</sup>, Philipp A. Neumann<sup>1</sup>, Rakieb Andargachew<sup>1</sup>, Jennifer C. Brazil<sup>1,2</sup>, Oscar Medina-Contreras<sup>1,2</sup>, Timothy L. Denning<sup>1,2</sup>, Asma Nusrat<sup>1</sup>, and Charles A. Parkos<sup>1,2</sup>

<sup>1</sup>Epithelial Pathobiology and Mucosal Inflammation Unit, Department of Pathology and Laboratory Medicine

<sup>2</sup>Department of Pediatrics, Emory University, Atlanta, Georgia 30322

### Abstract

Neutrophil transepithelial migration (TEM) during acute inflammation is associated with mucosal injury. Using models of acute mucosal injury in-vitro and in-vivo, we describe a new mechanism by which neutrophils infiltrating the intestinal mucosa disrupt epithelial homeostasis. We report that junctional adhesion molecule-like protein (JAML) is cleaved from neutrophil surface by zinc-metalloproteases during TEM. Neutrophil-derived soluble JAML bound to the epithelial tight junction protein coxsackie-adenovirus receptor (CAR) resulting in compromised barrier and inhibition of wound repair, through decreased epithelial proliferation. The deleterious effects of JAML on barrier and wound repair were reversed with an anti-JAML mAb that inhibits JAML-CAR binding. Thus, JAML released from transmigrating neutrophils across inflamed epithelia can promote recruitment of leukocytes and aid in clearance of invading microorganisms. However, sustained release of JAML under pathologic conditions associated with persistence of large numbers of infiltrated neutrophil would compromise intestinal barrier and inhibit mucosal healing. Targeting JAML-CAR interactions may thus improve mucosal healing responses under conditions of dysregulated neutrophil recruitment.

### Introduction

Many inflammatory conditions of mucosal surfaces are characterized by epithelial wounds in association with robust infiltration of neutrophils, or polymorphonuclear leukocytes (PMN). Examples include Crohn's disease and ulcerative colitis where recruitment of PMN into the intestinal lumen parallels mucosal ulceration and patient symptoms. Conversely,

Users may view, print, copy, and download text and data-mine the content in such documents, for the purposes of academic research, subject always to the full Conditions of use:[http://www.nature.com/authors/editorial\\_policies/license.html#terms](http://www.nature.com/authors/editorial_policies/license.html#terms)

Corresponding author: Charles Parkos M.D.,PhD., Emory University, Whitehead Biomedical Research Bldg, 105B, 615 Michael Street, Atlanta, GA 30322, Ph: 404-727-8536, Fax: 404-727-3321, cparkos@emory.edu.

\*These authors contributed equally to this work.

The authors declare no conflict of interests.

**Supplemental Figures:** Supplementary Material is linked to the online version of the paper at <http://www.nature.com/mi>. Table 1: Monoclonal antibodies to JAML do not cross-react with other CTX family. Supplemental Figure 1: Purified anti-JAML mAbs detect JAML in human myelomonocytic cells. Supplemental Figure 2: Human monocytes shed JAML upon activation with PMA.

resolution of PMN migration in these conditions is associated with mucosal healing and disease remission.

Sensing mucosal damage, PMN exit the microcirculation and migrate towards epithelial surfaces, driven by chemoattractants derived from invading organisms and resident cells that include bacterial peptides such as fMLF and chemokines such as IL-8 and heparin A3<sup>1-3</sup>. PMN TEM is regulated by a complex series of leukocyte adhesive interactions with endothelial cells, matrix components and epithelial cells. Receptor-ligand interactions that mediate migration of PMN across the epithelium are of particular importance given the association between disease symptoms and barrier dysfunction resulting from PMN transmigration.

Transmembrane receptors of the CTX (cortical thymocyte antigen of Xenopus) family of proteins expressed at intercellular junctions, including junctional adhesion molecules (JAMs), have been shown to regulate leukocyte interactions with endothelial and mucosal epithelial cells as well as epithelial cell homeostasis and barrier function<sup>4-7</sup>. A closely related JAM-like molecule, JAML<sup>8</sup> was reported to play a role in PMN TEM<sup>9</sup> through interaction with another CTX protein, coxsackie-adenovirus receptor (CAR) localized to the tight junction (TJ) in epithelia and certain endothelia<sup>9-11</sup>. Both JAML and CAR are type I glycoproteins containing two extracellular Ig-like domains, a single transmembrane helix, and a cytoplasmic tail with presumed signaling elements<sup>12</sup>. CAR is abundantly expressed in various epithelia and has been implicated in the regulation of epithelial permeability and cell adhesion to extracellular matrix, yet its function is incompletely understood<sup>9-11</sup>. JAML expression is restricted to PMN, monocytes and some T-cells<sup>8,13,14</sup> thus can mediate interactions with epithelial tight junctions through binding to CAR. In the skin, JAML was found to act as a costimulatory molecule for  $\gamma\delta$ T-cells. JAML binding to CAR expressed on keratinocytes induced increased T-cell proliferation and production of cytokines and growth factors<sup>14</sup>.

In this study, we investigated the biology of JAML in PMN, and the functional consequences of JAML interactions with epithelial CAR in wound healing. We show that JAML is shed from PMN as a soluble molecule during TEM. We report that ligation of epithelial CAR by shed JAML impairs epithelial barrier function and inhibits mucosal wound healing. We discuss these findings in the context of epithelial injury associated with acute mucosal inflammation.

## Results

### Role of JAML/CAR interactions in PMN adhesion to intestinal epithelium

CAR regulates epithelial barrier function while serving as a ligand for JAML on PMN<sup>9-11</sup>. To investigate the functional biology of JAML-CAR interactions during PMN TEM we generated monoclonal antibodies (mAbs) against the extracellular domain of human JAML (DW100, DW216). These mAbs specifically recognized JAML on PMN, monocytes and on differentiated promyelocytic cell lines, HL-60 and PLB-985 (Supplemental Figure 1), and did not cross-react with other related CTX family members (Supplemental Table 1). Both mAbs bound the membrane distal domain (sJAML.D1), but not the membrane proximal

domain (sJAML.D2) of JAML (Fig 1a). Since JAML binds to the membrane distal Ig like domain of CAR<sup>14</sup>, we tested whether these mAbs inhibited CAR-GST binding to immobilized sJAML-His. While, addition of DW100 prevented CAR-GST binding to JAML, DW216 had no effect (Fig 1b). Thus, DW100 and DW216 recognize two distinct epitopes on JAML-D1 domain and the DW100 epitope resides in close proximity/overlaps with the CAR binding site. Both DW100 (not shown) and DW216 (Fig 1c) immunoprecipitated a broad ~55-65kD protein band consistent with the size of full length JAML from lysates of surface biotinylated differentiated HL60 and PLB-985 cells.

To confirm functional inhibition of JAML-CAR interactions by mAb DW100, we quantified PMN adhesion to monolayers of intestinal epithelial cells (T84 or Caco-2) expressing high levels of CAR under Ca<sup>2+</sup> free conditions which served to open tight junctions and eliminate CD11b/CD18-dependent binding contributions. Addition of DW100 but not DW216 significantly inhibited PMN adhesion (~35%) to both T84 or Caco-2 monolayers (Figure 1d). Furthermore, stable knockdown of CAR expression in Caco-2 cells diminished adhesion of PMN to the level observed with addition of mAb DW100 (Fig 1d). Together these findings demonstrate that JAML-CAR interactions mediate PMN adhesion to intestinal epithelium.

### **PMN surface expression of JAML is lost during activation and transepithelial migration**

JAML-CAR interactions have been suggested to play a role in mediating PMN TEM, as soluble JAML and polyclonal JAML antiserum were reported to partially inhibit PMN TEM<sup>9</sup>. However, we observed a relatively minor inhibitory effect of mAb DW100 on PMN TEM (~15%), in contrast to major inhibition observed following inhibition of CD11b/CD18 (Supplemental Figure 2). We thus analyzed JAML expression on PMN following adhesion to epithelial cells and TEM. PMN adhesion to T84 monolayers resulted in partial loss of surface JAML (1.5-fold decrease, Fig 2a,e), compared to control PMN in suspension. Intriguingly, near complete loss of JAML expression was observed after PMN migration across T84 or Caco-2 (not shown) monolayers (Fig 2b,e). In contrast, surface expression of CD11b/CD18 after TEM was increased. We further tested whether JAML expression on PMN was lost during PMN transmigration across monolayers of endothelial cells (HDMECs) as has been observed for L-selectin. In contrast to the near complete loss observed during TEM, only a minor reduction of cell surface JAML was observed after transendothelial migration (Fig 2c,e).

Since PMN TEM is linked to chemoattractant-stimulated activation, we examined whether PMN stimulation in suspension was sufficient to induce the loss of JAML or whether PMN contact with epithelial cells was required. PMN incubation with 10nM fMLF had no significant effect on JAML expression (not shown), however treatment with 100nM fMLF resulted in partial but significant loss of JAML expression (2.4-fold decrease, Fig 2d/e). Moreover, treatment with the potent activating agent PMA (200nM), induced a near complete loss of cell surface JAML from PMN, suggesting that the loss of JAML was both stimulus and dose-dependent. In contrast, expression of CD18/CD11b was increased with both treatments indicative of PMN activation. Furthermore, loss of JAML upon activation with PMA was also observed in monocytes (Supplemental Figure 3). Interestingly, PMN

adhesion to epithelial monolayers in the absence of an additional activating stimulus also resulted in decreased JAML expression ( $\sim 1.5$ -fold), that was similar in magnitude to the decrease observed after migration across endothelial monolayers (Fig 2e). The loss of cell surface JAML after PMN TEM was further confirmed by immunofluorescence staining (Fig 2f). These data suggest that loss of JAML in myelomonocytic cells is activation-dependent and potentiated by contact with epithelial/endothelial cells during the transmigration response.

We next examined whether JAML expression is also lost *in vivo* during PMN recruitment into inflamed murine intestine. In these experiments PMN recruitment was induced by DSS-mediated mucosal injury and JAML expression was analyzed on PMN isolated from colonic lamina propria (colon PMN) and compared to PMN freshly isolated from blood by flow cytometry using a hamster anti-murine JAML mAb<sup>14</sup>. As observed with human PMN *in vitro*, while JAML expression was detected on circulating murine PMN, it was lost on PMN isolated from the lamina propria of inflamed colons (Fig 2g, left panels). Given a recent report documenting JAML expression on the surface of  $\gamma\delta$ T cells<sup>14</sup>, we compared the PMN JAML expression results with those on  $\gamma\delta$ T cells. JAML expression was unchanged on both circulating and colonic lamina propria  $\gamma\delta$ T cells (Fig 2g). We further confirmed that PMA-induced activation of lamina propria  $\gamma\delta$ T cells had no effect on surface expression of JAML (Supplemental Figure 4). Together these findings suggest that JAML shedding during migration into the colon is specific to myelomonocytic cells.

### **JAML is cleaved from the PMN surface during TEM by Zinc-dependent metalloproteases**

Given the findings highlighted above, we hypothesized that the observed loss of cell-associated JAML during PMN activation was due to ectodomain shedding. To test this, mAbs DW100 and DW216 were used in a sandwich ELISA to capture and detect shed JAML ectodomains in cell-free supernatants. JAML was detected in supernatants from both PMA-activated PMN and differentiated PMN-like cell lines HL60 and PLB-985 (Fig 3a). Upon activation PMN are known to release membrane-bound microparticles/ectosomes from the cell surface<sup>15</sup>, thus we measured the levels of JAML in supernatants from activated cells after high speed ultracentrifugation (100K $\times$ g). No changes in the levels of JAML were observed, indicating that JAML is shed as a soluble molecule upon PMN activation (data not shown). Furthermore, the cleaved portion of JAML was immunoprecipitated from supernatants of biotin-labeled, PMA-stimulated PLB-985 cells and detected as a protein of  $\sim 45$ KD (Fig 3b), consistent with the size of JAML extracellular domain (full size is  $\sim 55$ -65kD, Fig 1c). To determine if JAML release from activated leukocytes was dependent on cellular proteases, we stimulated differentiated PLB-985 cells with PMA in the presence or absence of a variety of protease inhibitors, and assayed for JAML in cell supernatants. A mixture of serine, cysteine and several other protease inhibitors, as well as thrombin and serine protease inhibitors, AEBSF or N-Ethyl maleimide failed to inhibit JAML shedding (data not shown). However, inhibition of Zn<sup>++</sup> dependent metalloproteases with either phenanthroline, or TNF $\alpha$  protease inhibitor-2 (TAPI-2)<sup>16,17</sup>, significantly decreased cellular release of JAML after PMA activation (Fig 3c). This inhibition of JAML shedding was verified by FACS staining of differentiated PLB-985 cells with mAb DW216 (Fig 3d). While the possibility of further protease-dependent cleavage of JAML cannot be excluded,

the above findings suggest that a fragment of JAML consisting of the majority of the extracellular domain is released from the surface of activated PMN in a Zn<sup>++</sup> metalloprotease-dependent manner.

### Soluble JAML binds to epithelial CAR and inhibits epithelial barrier function

To examine whether JAML released from PMA-activated PMN was biologically active and was able to bind CAR, CHO-K1 cells stably expressing CAR (CHO-CAR) were incubated with supernatants from PMA-stimulated PMN (200nM) and JAML binding to CAR was confirmed by flow cytometry and confocal microscopy (Fig 4a,b). PMA treatment alone (200nM) had no effect on the expression of CAR on CHO-CAR cells (not shown). To further investigate the biological effects of JAML ectodomains on epithelial barrier function without the adverse effects of PMN stimulating agents such as PMA, we generated soluble, recombinant JAML (sJAML) and confirmed its binding to CAR on CHO-CAR cells, (Fig 4c, left panel). Similarly, we show the binding of soluble recombinant CAR to JAML stably expressed in CHO cells (CHO-JAML, Fig 4d, left panel). In both experimental setups JAML-CAR binding was inhibited by DW100, but not DW216 (Fig 4c,d, right panels), confirming the inhibitory function of DW100. Furthermore, using immunofluorescence labeling, we confirmed binding of sJAML to T84 epithelial cell monolayers, where it was found to colocalize with CAR (Fig 4e, upper panels). Addition of DW100 prevented these interactions (Fig 4e, bottom panels). Since CAR has been implicated in the regulation of TJ assembly and epithelial barrier function<sup>18</sup>, we hypothesized that JAML released from migrating or activated PMN during inflammation may alter epithelial barrier function through binding to CAR. We examined the effects of sJAML on epithelial barrier recovery after Ca<sup>2+</sup> switch assays by measuring transepithelial resistance (TER) and FITC-dextran flux (3kDa) as previously described<sup>19</sup>. Addition of sJAML, but not SIRP- $\alpha$  (binds a basolaterally expressed epithelial ligand CD47<sup>20</sup>), significantly delayed recovery of barrier function as measured by TER (Fig 4f). Compromised epithelial barrier function in the presence of sJAML was still evident after 24h, as confirmed by 9-fold increase in dextran flux (Fig 4g). Importantly, inhibition of JAML-CAR binding with DW100, but not DW216 (not shown) mAb reversed these effects.

### JAML-CAR interactions result in inhibition of intestinal epithelial wound healing

PMN TEM is often associated with epithelial injury, we thus examined whether JAML-CAR binding influenced epithelial wound repair using *in vitro* scratch wound resealing assays. Addition of sJAML to scratch wounded monolayers significantly delayed wound closure (~30%) 48 and 72 hours after injury (Fig 5a). Importantly, in the presence of DW100 but not DW216 sJAML-mediated inhibition of wound closure was reversed (Fig 5a).

It is accepted that epithelial cell migration mediates wound closure within the first 24 hours of injury<sup>21</sup>. However, we observed that sJAML had relatively minor inhibitory effects on wound closure within the first day suggesting that JAML binding to CAR affected cell proliferation rather than epithelial migration. Indeed using Edu incorporation assay<sup>22</sup>, we found that addition of sJAML (24h) to wounded T84 monolayers significantly decreased proliferation of cells at wound edges from 38.4 $\pm$ 1.8% to 24.1 $\pm$ 2.1% of Edu positive cells, (Fig 5b and representative images, Fig 5c), however did not affect proliferation of cells

remote from wounded areas (Supplemental Figure 5d). Consistent with the wound healing results addition of DW100 but not DW216 (not shown) prevented the sJAML-dependent decrease in cell proliferation (Fig 5b). These findings suggest that the inhibitory effect of sJAML is dependent on access to CAR at tight junctions, which is enhanced after loss of epithelial cell-cell contacts, as occurs after injury. We further observed that addition of sJAML to subconfluent epithelial cell monolayers also significantly decreased cell proliferation which was reversed by DW100 but not DW216 (Supplemental Figure 5e,f). These observations suggest that sJAML-mediated inhibitory effects are not restricted to wound edges.

Using TUNEL staining we found no effect of sJAML on epithelial cell apoptosis, thus ruling out the potential contribution for cell apoptosis in sJAML-mediated inhibition of epithelial wound healing (not shown). Consistent with the sJAML-mediated decrease in epithelial cell proliferation, addition of sJAML to wounded IEC monolayers significantly attenuated wound-stimulated increases in phosphorylation of both c-Raf and Erk, which are key regulators of epithelial cell proliferation<sup>23</sup> (Fig 5d). Confirming the specificity of these responses to sJAML, the observed effects were reversed in the presence of DW100 mAb (Supplemental Figure 5a-c). In contrast, sJAML had no effect on phosphorylation of Akt as well as  $\beta$ -catenin (not shown). Together, these findings suggest that ligation of CAR by sJAML inhibits epithelial cell proliferation leading to impaired epithelial wound healing.

### **Ligation of CAR by sJAML or adenovirus protein Ad5 inhibits mucosal wound healing in vivo**

To extend the *in vitro* observations suggesting that binding of soluble JAML to CAR inhibits wound healing, we used a colonoscopic biopsy wound injury model in mice to examine the effects of CAR ligation on mucosal wound healing in-vivo. We took advantage of another CAR ligand, adenoviral fiber knob protein 5 (Ad5) that has been shown previously to bind human and murine CAR with high affinity<sup>14,24,25</sup>, and compete with JAML for CAR at the same binding site<sup>14</sup>. Ad5, but not Ad11 (related adenoviral fiber knob control that does not bind to CAR) bound to immobilized human CAR and to CHO cells transfected with CAR, and to CAR-expressing murine intestinal epithelial cell line (CMT). Furthermore, Ad5 but not Ad11 inhibited binding of murine sJAML to CMT cells (Fig 6a) confirming that Ad5 binds to the same or overlapping epitope as JAML on CAR. Consistent with these results, addition of Ad5 but not Ad11 to both human (T84) and murine (CMT) intestinal epithelial monolayers significantly inhibited wound closure (Fig 6b,c respectively) in a fashion similar to inhibitory effects observed with sJAML. Importantly, intraperitoneal administration of sJAML and recombinant Ad5 *in vivo* (20 $\mu$ g and 10 $\mu$ g, respectively twice daily) significantly inhibited colonic mucosal wound healing (4 days after wounding) compared to Ad11 or PBS alone (33 $\pm$ 4.2% and 24.3 $\pm$ 3.1% vs. 65.2 $\pm$ 2.7 and 66.7 $\pm$ 3.2%, respectively, Fig 6d). In these experiments, superficial colonic mucosal wounds were induced in mice treated with Ad5, Ad11 or PBS using a mouse colonoscope as previously described<sup>26</sup>. Healing of mucosal wounds was monitored 2 and 4 days post wounding by endoscopic imaging. Delayed wound closure was evident from histological analysis and whole mount preparations of wounded mucosa (Fig 6e left and middle panels, respectively). Furthermore, immunofluorescence labeling of frozen sections from harvested colonic

mucosal wounds (day 4 after wounding) confirmed colocalization of Ad5 but not Ad11 with epithelial CAR in wounded areas (Fig 6e, right panels).

### **Deleterious effects of PMN-derived JAML on epithelial wound repair are reversed by inhibition of JAML/CAR interactions**

We have shown that PMN activation, adhesion to and migration across intestinal epithelium leads to shedding of JAML. Thus we examined the direct effect of soluble JAML released from PMN on intestinal epithelial wound repair. PMN were applied to epithelial cell monolayers after introduction of linear scratch wounds and healing was assessed. Addition of PMN resulted in significant inhibition of wound closure (~40%) after 48 and 72 hours (Fig 7a). Importantly, anti-JAML mAb DW100 but not DW216 blocked a majority of PMN-dependent inhibitory effects on wound closure, confirming a major role for interactions between PMN-derived JAML with CAR in the regulation of intestinal epithelial wound healing (Fig 7a) and representative images Fig 7b). Together, these data indicate that JAML released from migrating leukocytes inhibits CAR-mediated regulation of intestinal epithelial wound healing under inflammatory conditions. Furthermore, inhibition of JAML-CAR interactions may be exploited therapeutically to improve healing responses under conditions of acute PMN recruitment to mucosal surfaces. From the above findings, we propose a model that highlights the role of shed JAML in the regulation of intestinal epithelial homeostasis under conditions of acute mucosal inflammation/injury (Fig 8).

## **Discussion**

In the active phases of many mucosal inflammatory conditions, PMN TEM is associated with increased epithelial permeability, tissue damage and patient symptoms. There are numerous reports detailing mechanisms by which high density PMN trafficking across mucosal surfaces results in altered barrier function and epithelial homeostasis. During TEM, subepithelial PMN initiate contact-dependent epithelial signaling events that result in protease activated receptor-mediated alterations in barrier function<sup>27</sup>. Additionally, proteases released by PMN, including elastase and cathepsin G have been shown to disrupt E-cadherin based epithelial cell-cell contacts<sup>28,29</sup> while also inducing junctional discontinuities<sup>30</sup>. Given these observations, it is not surprising that migration of large numbers of PMN across the epithelium results in sizeable discontinuities or ulcers/erosions<sup>31</sup>. Here, we report a new mechanism by which JAML shed from activated PMN during TEM binds to the TJ protein CAR resulting in signaling events that alter epithelial function. Specifically, we demonstrate that sJAML interaction with CAR significantly impairs epithelial barrier function and wound healing. We speculate that during the early phases of an acute inflammatory response JAML shedding may serve to facilitate efficient recruitment of additional leukocytes to the sites on injury or infection by delaying barrier recovery. One could envision this mechanism acting to facilitate simultaneous influx of large numbers of PMN en-masse rather than recruitment of single PMN that would have to individually unzip junctions and squeeze between adjacent epithelial cells to get into the intestinal lumen. While the above mechanism would provide an efficient way to quickly clear enteric infections, resolution of the acute inflammatory response would be a necessary and vital component needed to restore mucosal homeostasis. Interestingly, failure to clear massive numbers of infiltrated

PMN is observed in medically refractive ulcerative colitis, and under these pathologic conditions, sustained release of JAML could be linked to continued mucosal injury, ulceration and patient symptoms.

Other distinguishing features of JAML include an unconventional extracellular structure resulting from rigid assembly of the Ig domains and an extended, flexible stalk<sup>12</sup>. Such structure presumably facilitates unique interactions with CAR on the surface of epithelial cells. Ligand binding is mediated by the membrane distal Ig-like domain of JAML (JAML.D1) and, as shown in this report, is completely inhibited by a D1 binding mAb (DW100) (Fig 1). By contrast, another anti-JAML D1 mAb DW216 did not affect JAML binding to CAR.

Using anti-JAML mAbs, we report that JAML expression on PMN and monocytes is decreased/lost after activation with fMLF and PMA and that the loss of JAML correlates with the degree of PMN activation and nature of the given stimulus. Interestingly, using polyclonal antiserum raised against sJAML-Fc, we previously reported increased staining in activated PMN<sup>9</sup>. However, while producing anti-JAML specific mAbs, we identified antibodies with cross reactivity to other JAM proteins. Thus, binding of polyclonal anti-JAML antiserum to related molecules may have contributed to such findings. As shown in Supplemental Table 1, the anti-JAML mAbs in this report do not cross react with other related JAM proteins. Additionally, in the current study, we report dose and agonist-dependent shedding of JAML that requires zinc-dependent metalloprotease activity in PMN. Thus, priming of PMN during isolation coupled with differences in activation of metalloproteases may affect cell-surface JAML expression and PMN function. Indeed, addition of the zinc-dependent metalloprotease inhibitor TAPI-2 to suspensions of PMN not only inhibits shedding of JAML but also significantly increases JAML-dependent PMN transepithelial migration that is specifically blocked by DW100. Given this observation one might thus ask whether JAML shedding during PMN activation may act as a brake and reduce TEM. In the case of luminal antigen/bacterial leakage into the lamina propria, it might be advantageous for recruited PMN to be retained in the subepithelial space to clear microbes locally, rather than migrating into the lumen. However, we have shown that CD11b/CD18 is by far the dominant regulator of PMN-epithelial adhesion/transmigration and that blockage of JAML under conditions supporting CD11b/CD18-mediated migration has only minor effects on PMN TEM. Interpretation of experiments testing if JAML shedding is directly associated with decreased PMN TEM are confounded by other factors secondary to PMN activation, so contributions from JAML loss in this context remain unclear. Alternatively, it is possible that conditions resulting in diminished zinc-dependent metalloproteinase activity could enhance PMN migration and further augment the inflammatory response at the level of the epithelium.

Zinc metalloproteases mediate cleavage of L-selectin from the PMN surface<sup>32</sup> during early PMN rolling on vascular endothelium<sup>33</sup>. In contrast, JAML was mostly retained on PMN surface following transendothelial migration and was cleaved during TEM. Perhaps such activation is linked to the level of CAR expression which has been shown to be low and variable in different endothelia<sup>34,35</sup>, but highly expressed on intestinal and other types of epithelial cells. Given the strong association of JAML cleavage with TEM, the shed



ectodomains would be in intimate contact with epithelial cells, and by binding to CAR, could affect epithelial function in a paracrine manner. Such findings also likely apply to monocytes as we and others<sup>13</sup> have observed significant levels of JAML expression on monocytes, and our studies show that monocyte-associated JAML is also lost upon activation. Given that monocytes are also critical in the innate immune response and represent early arrivers to sites of mucosal inflammation, one can envision these innate immune cells as an additional source of released JAML ectodomains that could amplify PMN-mediated effects on epithelial function.

In this report we demonstrate that the shed/soluble JAML ectodomain inhibits epithelial barrier function and wound healing. It is well established that epithelial wound healing involves enhanced directional polarization and migration of cells at the leading edge, followed by increased cell proliferation at later time points<sup>21</sup>. Our results suggest that interactions between JAML and CAR delay intestinal epithelial wound closure by inhibiting cell proliferation. After probing candidate signaling pathways, we found that sJAML inhibition of wound closure is mediated by decreased ERK signaling, a key pathway known to be involved in the regulation of epithelial cell proliferation<sup>23,36</sup>.

A recent study showed beneficial effects of JAML-CAR interactions on dermal wound healing mediated by activation of JAML on  $\gamma\delta$ T cells in mouse skin. In that study, it was shown that  $\gamma\delta$ T cell interactions with keratinocytes mediated through JAML-CAR binding resulted in JAML-mediated T cell proliferation along with production of T cell-derived cytokines and keratinocyte growth factor, which proved to enhance dermal wound closure<sup>14</sup>. These observations highlight signaling events secondary to JAML-CAR binding that are cell-type and context-specific. While ligation of JAML expressed on T cells in the skin results in T cell-derived pro-restitutive responses, in this study, we show that JAML-mediated ligation of CAR expressed on epithelial cells in the intestine results in epithelial-derived inhibitory restitutive responses. While the role of JAML in PMN function is not clear, it is most certainly distinct from that reported in T cells. One notable difference highlighted in figure 2g of this study demonstrates no change in JAML expression on  $\gamma\delta$ T cells isolated from the colonic lamina propria during colitis, or following direct activation with PMA (Supplemental Figure 4), which has been previously shown to activate Zn<sup>++</sup>-dependent metalloproteases<sup>37</sup>. These findings suggest that, unlike PMN and monocytes, T cells do not shed JAML upon infiltration of the colonic mucosa. During acute mucosal inflammation, one could envision significant amounts of soluble JAML released in the immediate vicinity of high-density PMN migration. Ligation of epithelial CAR under these circumstances would likely have a pro-inflammatory effect. Similarly, the findings in this report raise the question of whether PMN-derived JAML might play a role in poor healing of mucosal ulcers associated with massive PMN infiltration in conditions such as ulcerative colitis.

Given known functions of related CTX family members, it is reasonable to propose that CAR ligation by JAML mediates outside-in signaling to affect multiple cellular functions. For example, studies on a closely related TJ protein JAM-A have revealed that homodimerization in the membrane distal D1-domain results in close apposition of cytoplasmic scaffold molecules to facilitate signaling events. JAM-A dimerization enhances

Rap1-mediated effects on cell migration via control of cell surface  $\beta$ 1-integrin levels<sup>38,39</sup>. JAM-A dimerization has also been shown to regulate epithelial cell proliferation by Akt,  $\beta$ -catenin signaling pathways<sup>6</sup>. CAR that is expressed at epithelial TJs, colocalizes with the cytoplasmic plaque protein zonula occludens-1 (ZO-1)<sup>11</sup>. While CAR is mainly recognized as the receptor that mediates coxsackie-adenovirus attachment<sup>40,41</sup>, like JAM-A, it has also been reported to play a role in the regulation of epithelial permeability and TJ reassembly. Addition of soluble CAR to intestinal epithelial monolayers after  $\text{Ca}^{2+}$  switch assay has been shown to inhibit TJ reassembly<sup>11</sup>. Like JAM-A, CAR has been reported to dimerize *in cis*<sup>42</sup> in the D1 domain which is also a presumed binding domain for JAML<sup>12</sup>. It is thus possible that JAML binding may inhibit CAR-CAR dimerization, altering downstream signaling events.

In summary, we present a model in figure 8 highlighting acute PMN recruitment by mucosal inflammatory cues resulting in shedding of a majority of cell surface JAML during TEM. Shed JAML molecules bind TJ-associated CAR and alter signaling events resulting in perturbed barrier function and inhibition of epithelial cell proliferation leading to impaired wound closure. While such responses may serve to enhance the early phases of acute mucosal inflammatory responses, they may also be responsible for poorly healing mucosal ulcers associated with massive PMN infiltration in conditions such as ulcerative colitis. Development of novel therapeutics that specifically block JAML-CAR receptor-ligand interactions in the intestine may have significant value in promoting barrier function and epithelial wound closure under conditions associated with pathologic accumulation of neutrophils in the mucosa.

## Material and Methods

### Cells

HL60, wild type Chinese hamster ovary cells (CHO) and HEK293T human embryonic kidney cell line were obtained from ATCC. HL60 and PLB-985<sup>43,44</sup> were passaged in RPMI containing 20% heat inactivated FBS (Atlanta Biologicals) with supplements and differentiated as previously described<sup>44</sup>. CHO-K1, HEK293T cells, Caco-2 and T84 epithelial cell lines were cultured as described<sup>45</sup>. HDMEC, human dermal microvascular endothelial cells (passage 4-9) were a kind gift from Dr. Nancy Louis. Human blood was drawn and handled according to protocols for the protection of human subjects, as approved by the Emory University Hospital Institutional Review Board, and in accordance with the Declaration of Helsinki (2000). PMN were isolated by density gradient centrifugation<sup>45</sup>.

### Generation of recombinant proteins

All plasmid constructs were generated by the Custom Cloning Center Facility at Emory University and sequences confirmed. Human JAML (GenBank: AJ515553.2) was cloned in pcDNA3.0 (Invitrogen Life Technologies) with C-terminal His-tags or 6XMyC or rabbit-Fc<sup>20</sup>. The extracellular domains of JAML were tagged after residue Leu<sup>259</sup> for JAML.D1D2-His (sJAML), and Pro<sup>140</sup> for sJAML.D1. CHO or HEK293 T cells were transfected using polyethylenimine (*PEI*), and stable clones selected with G418/HygromycinB appropriately. Soluble His-tagged proteins were purified on Ni-NTA agarose

beads (Qiagen, Valencia, CA). Soluble CAR-GST construct has been described<sup>9</sup>. Full-length CAR and JAML constructs were expressed in CHO cells (CHO-CAR or CHO-JAML) and expression assessed by flow cytometry. Adenoviral knob proteins Ad5-His (Ad5) and Ad11-His (Ad11) were expressed in E.Coli from respective constructs (a kind gift of Dr. G. Nemerow, Scripps Institute, LaJolla,CA). Soluble murine JAML-mFc construct was cloned into pVL1393 (Invitrogen), expressed in the Baculovirus system (Invitrogen) and purified on Protein A Sepharose.

### Antibodies and reagents

RmcB and 9E10 were purified from hybridomas. Anti-CD11b/CD18 (CBRM1/29) was previously described<sup>46</sup>. Anti-human CAR (H-300) from Santa Cruz (Santa Cruz, CA). Murine PMN and  $\gamma\delta$ T cells: CD3 $\epsilon$ eFluor450 (eBio500A2), CD45-PerCP-Cy5.5 (RM4-5), TCR $\gamma\delta$ -FITC (GL3), Gr1-APC-eFluor780 (RB6-8C5), B220-APC (RA3-6B2) from BD Biosciences, and JAML-PE (4E10; BioLegend). Mouse-Alexa488 and rabbit-Alexa555 (Invitrogen, Carlsbad, CA), rabbit anti-Phospho-cRaf and Phospho-p44/42 MAPK (Erk 1/2) (Cell Signaling, Danvers, MA), mouse-HRP IgG, goat anti-rabbit IgG (Jackson Immunoresearch, West Grove, PA). HRP-conjugated anti-GST (GE Healthcare), murine anti-His (Abcam, Cambridge, MA) and HRP-conjugated Streptavidin (Zymed, San Francisco, CA). Antibodies were biotinylated using Ezlink Sulfo-NHS-LC-Biotin (Thermo Scientific, Rockford, IL) or conjugated to CNBr-Sepharose 4 Fast Flow beads (GE Healthcare) according to manufacturers instructions. ABTS, (2,2'-azinobis-(3-ethylbenzothiazoline-6-sulfonic acid), Phenanthroline monohydrate, N-Ethylmaleimide, Phenylmethylsulfonyl fluoride (PMSF), protease inhibitor cocktail (#P8340), PMSF, Phorbol Myristate Acetate (PMA), HBSS with/without  $\text{Ca}^{2+}$  and  $\text{Mg}^{2+}$  ( $\text{H}^+/\text{H}^-$ ), fMLF and phosphatase inhibitors cocktails 1 and 2, Sigma (St Louis, MO). TNF $\alpha$  protease inhibitor-2 (TAPI-2) Calbiochem (Merk, Darmstadt, Germany).

### Surface biotinylation, immunoprecipitation and immunoblotting

HL60, PLB-985 cells or PMN were washed, resuspended in  $\text{H}^+$  at  $5 \times 10^7/\text{ml}$  and incubated with 8 mg Ezlink Sulfo-NHS-LC-Biotin dissolved in 1 ml PBS (30 min. 4°C). After quenching in 20ml 40mM Tris-HCl pH 8.0, 100mM NaCl, cell lysates were prepared for immunoprecipitation and immunoblotting as described<sup>6</sup>.

### Detection of soluble JAML by capture ELISA

Immulon II microtiter plates were coated with mAb DW100 (1 $\mu\text{g}/\text{well}$ , overnight. at 4°C), then blocked with 5% Roche blocking reagent and incubated with supernatants of stimulated PMN, HL60 or PLB-985 as well as serial dilutions of purified sJAML (100 $\mu\text{l}$ , 1hr, RT). After washing, biotinylated-DW216 (10 $\mu\text{g}/\text{ml}$ ) was added followed by incubation with streptavidin-HRP. Binding was analyzed in a microplate reader at 405nm after addition of ABTS.

### CAR binding assay

Immulon II plates were coated with sJAML (10 $\mu\text{g}/\text{ml}$  in PBS, overnight at 4°C) and blocked as described above. CAR-GST (10 $\mu\text{g}/\text{ml}$  in 100 $\mu\text{l}$ , 1hr RT) was added to wells in the

presence of antibody solutions (10 $\mu$ l, 1hr, RT) followed by goat anti-GST-HRP and ABTS as above.

### Cell Isolation and FACS staining

Isolation of blood and lamina propria cells was performed as previously described<sup>47</sup>. Following Fc receptors block ( $\alpha$ -Fc $\gamma$ RIII/II, 2.4G2) cells were prepared for flow cytometry and analyzed using LSR II Cytometer. CD45<sup>+</sup> live cells were gated and cell populations were defined as follows: CD3 $\epsilon$ <sup>+</sup> TCR $\gamma\delta$ <sup>+</sup> cells ( $\gamma\delta$ T cells), Gr1<sup>+</sup>B220<sup>-</sup> (neutrophils) and Gr1<sup>-</sup>B220<sup>+</sup> (B cells). To analyze JAML expression on PMN adherent to T84 epithelial cell, PMN (2.5 $\times$ 10<sup>5</sup> cells/well) were applied to T84 monolayers (15min), harvested with trypsin/EDTA and stained as previously described<sup>9</sup>, gating on CD18/CD11b positive cells. MFI represents the mean fluorescence intensity minus the mean fluorescence intensity of IgG control.

### Cell adhesion assay

Intestinal epithelial cells (T84/Caco-2) were seeded on 24-well plates (1 $\times$ 10<sup>6</sup> cells/well) and cultured to confluency. PMN or HL60 cells were loaded with CellTracker<sup>TM</sup> Green (CMFDA, 10 min at 37 $^{\circ}$ C) and added to wells (2.5 $\times$ 10<sup>5</sup> cell/well) for 1 hour (in the absence of extracellular Ca<sup>2+</sup>, (to open up junctions) at 37 $^{\circ}$ C. After washing, adherent PMN were lysed with 1% TritonX-100. Fluorescence intensity was measured using FluoStar Galaxy plate reader at excitation/emission wavelengths of 485/535 nm. Data are presented as relative fluorescence intensity minus background fluorescence of epithelial monolayer alone.

### Immunofluorescence microscopy

PMN and epithelial cells were immunofluorescently stained using standard protocols as previously described<sup>27</sup>. All images were acquired on a LSM 510 confocal microscope (Carl Zeiss, Thornwood, NY) with Plan-Neofluor 60 $\times$  and 40 $\times$  objectives.

### Assessment of cell proliferation and apoptosis

Epithelial cell proliferation and apoptosis were assessed using Click-iT EdU Alexa 488 cell proliferation kit (Invitrogen) and Tunel staining (In Situ Cell Death Detection Kit, Roche, Mannheim, Germany) respectively. Monolayers were incubated for 24 hr at 37 $^{\circ}$ C before addition of EdU or In Situ Cell Death Detection kits. 5 random fields/condition were analyzed and data presented as % proliferating/apoptotic cells in each field.

### Epithelial wound closure assays

Wounds were introduced to confluent T84 and Caco-2 monolayers and monitored as previously described<sup>48</sup>. *Colonoscopy in live mice*: Superficial wounds were introduced *in vivo* (mouse colon) using colonoscopic biopsy techniques as described<sup>26</sup>. PBS (100 $\mu$ l), Ad5 (10 $\mu$ g/100 $\mu$ l) Ad11 (10 $\mu$ g/100 $\mu$ l) or sJAML (20 $\mu$ g/100 $\mu$ l) were administered ip twice daily. All procedures were approved by the Emory University IACUC and performed according to NIH criteria.

## DSS treatment

Mice were fed with 3% DSS (wt/vol; MP Biomedicals) for 5 days, and assessed as previously described<sup>49</sup>.

## Statistics

Statistical significance was assessed by a Student t-test or by one way ANOVA with a Newman-Keuls Multiple Comparison Test using Graphpad Prism (V4.0), and set at  $P < 0.05$ .

## Supplementary Material

Refer to Web version on PubMed Central for supplementary material.

## Acknowledgments

We thank Emory DDRDC core facility technical support in culturing intestinal epithelial cell lines (supported by funding from NIH DK064399). We also thank Dr. Oskar Laur and the Custom Cloning Center Facility at Emory University for the generation of JAML constructs. This work was supported in part by grants from the NIH (DK072564, DK061379, DK079392, DK055679, DK059888), trainee support from the NIH (DK007771), Career Development Award from the CCFA to Dr. Ronen Sumagin (CCFA3597).

## References

1. Rhee SH, Keates AC, Moyer MP, Pothoulakis C. MEK is a key modulator for TLR5-induced interleukin-8 and MIP3 alpha gene expression in non-transformed human colonic epithelial cells. *Journal of Biological Chemistry*. 2004; 279:25179–25188. [PubMed: 15069060]
2. MacDermott RP, Sanderson IR, Reinecker HC. The central role of chemokines (chemotactic cytokines) in the immunopathogenesis of ulcerative colitis and Crohn's disease. *Inflammatory Bowel Diseases*. 1998; 4:54–67. [PubMed: 9552229]
3. Mrsny RJ, et al. Identification of heparin sulfate 3 in inflammatory events: a required role in neutrophil migration across intestinal epithelia. *Proc Natl Acad Sci U S A*. 2004; 101:7421–7426. [PubMed: 15123795]
4. Nourshargh S, Krombach F, Dejana E. The role of JAM-A and PECAM-1 in modulating leukocyte infiltration in inflamed and ischemic tissues. *J Leukoc Biol*. 2006; 80:714–718. [PubMed: 16857733]
5. Laukoetter MG, et al. JAM-A regulates permeability and inflammation in the intestine in vivo. *Journal of Experimental Medicine*. 2007; 204:3067–3076. [PubMed: 18039951]
6. Nava P, et al. JAM-A regulates epithelial proliferation through Akt/beta-catenin signalling. *Embo Reports*. 2011; 12:314–320. [PubMed: 21372850]
7. Severson EA, et al. Cis-dimerization mediates function of junctional adhesion molecule A. *Molecular Biology of the Cell*. 2008; 19:1862–1872. [PubMed: 18272784]
8. Moog-Lutz C, et al. JAML, a novel protein with characteristics of a junctional adhesion molecule, is induced during differentiation of myeloid leukemia cells. *Blood*. 2003; 102:3371–3378. [PubMed: 12869515]
9. Zen K, et al. Neutrophil migration across tight junctions is mediated by adhesive interactions between epithelial coxsackie and adenovirus receptor and a junctional adhesion molecule-like protein on neutrophils. *Mol Biol Cell*. 2005; 16:2694–2703. [PubMed: 15800062]
10. Raschperger E, et al. The coxsackie- and adenovirus receptor (CAR) is an in vivo marker for epithelial tight junctions, with a potential role in regulating permeability and tissue homeostasis. *Experimental Cell Research*. 2006; 312:1566–1580. [PubMed: 16542650]
11. Cohen CJ, et al. The coxsackievirus and adenovirus receptor is a transmembrane component of the tight junction. *Proceedings of the National Academy of Sciences of the United States of America*. 2001; 98:15191–15196. [PubMed: 11734628]

12. Verdino P, Witherden DA, Havran WL, Wilson IA. The Molecular Interaction of CAR and JAML Recruits the Central Cell Signal Transducer PI3K. *Science*. 2010; 329:1210–1214. [PubMed: 20813955]
13. Luissint AC, Lutz PG, Calderwood DA, Couraud PO, Bourdoulous S. JAM-L-mediated leukocyte adhesion to endothelial cells is regulated in cis by alpha4beta1 integrin activation. *J Cell Biol*. 2008; 183:1159–1173. [PubMed: 19064666]
14. Witherden DA, et al. The junctional adhesion molecule JAML is a costimulatory receptor for epithelial gammadelta T cell activation. *Science*. 2010; 329:1205–1210. [PubMed: 20813954]
15. Eken C, et al. Polymorphonuclear neutrophil-derived ectosomes interfere with the maturation of monocyte-derived dendritic cells. *J Immunol*. 2008; 180:817–824. [PubMed: 18178820]
16. Ludeman MJ, Zheng YW, Ishii K, Coughlin SR. Regulated shedding of PAR1 N-terminal exodomain from endothelial cells. *Journal of Biological Chemistry*. 2004; 279:18592–18599. [PubMed: 14982936]
17. Le Gall SM, Auger R, Dreux C, Mauduit P. Regulated cell surface pro-EGF ectodomain shedding is a zinc metalloprotease-dependent process. *J Biol Chem*. 2003; 278:45255–45268. [PubMed: 12947092]
18. Koizumi JI, et al. Protein kinase C enhances tight junction barrier function of human nasal epithelial cells in primary culture by transcriptional regulation. *Molecular Pharmacology*. 2008; 74:432–442. [PubMed: 18477669]
19. Ivanov AI, et al. Microtubules regulate disassembly of epithelial apical junctions. *BMC Cell Biol*. 2006; 7:12. [PubMed: 16509970]
20. Lee WY, et al. Novel structural determinants on SIRP alpha that mediate binding to CD47. *J Immunol*. 2007; 179:7741–7750. [PubMed: 18025220]
21. Hopkins AM, et al. Organized migration of epithelial cells requires control of adhesion and protrusion through Rho kinase effectors. *American Journal of Physiology-Gastrointestinal and Liver Physiology*. 2007; 292:G806–G817. [PubMed: 17138966]
22. Salic A, Mitchison TJ. A chemical method for fast and sensitive detection of DNA synthesis in vivo. *Proc Natl Acad Sci U S A*. 2008; 105:2415–2420. [PubMed: 18272492]
23. Si H, et al. RNAi-mediated knockdown of ERK1/2 inhibits cell proliferation and invasion and increases chemosensitivity to cisplatin in human osteosarcoma U2-OS cells in vitro. *Int J Oncol*. 2012; 40:1291–1297. [PubMed: 22179790]
24. Bergelson JM, et al. Isolation of a common receptor for Coxsackie B viruses and adenoviruses 2 and 5. *Science*. 1997; 275:1320–1323. [PubMed: 9036860]
25. Kirby I, et al. Identification of contact residues and definition of the CAR-binding site of adenovirus type 5 fiber protein. *J Virol*. 2000; 74:2804–2813. [PubMed: 10684297]
26. Becker C, Fantini MC, Neurath MF. High resolution colonoscopy in live mice. *Nat Protoc*. 2006; 1:2900–2904. [PubMed: 17406549]
27. Chin AC, Lee WY, Nusrat A, Vergnolle N, Parkos CA. Neutrophil-mediated activation of epithelial protease-activated receptors -1 and -2 regulates barrier function and transepithelial migration. *Journal of Immunology*. 2008; 181:5702–5710.
28. Mayerle J, et al. Extracellular cleavage of E-cadherin by leukocyte elastase during acute experimental pancreatitis in rats. *Gastroenterology*. 2005; 129:1251–1267. [PubMed: 16230078]
29. Zemans RL, et al. Neutrophil transmigration triggers repair of the lung epithelium via beta-catenin signaling. *Proc Natl Acad Sci U S A*. 2011; 108:15990–15995. [PubMed: 21880956]
30. Rochat T, Casale J, Hunninghake GW, Peterson MW. Neutrophil cathepsin G increases permeability of cultured type II pneumocytes. *Am J Physiol*. 1988; 255:C603–611. [PubMed: 3142269]
31. Nusrat A, Parkos CA, Liang TW, Carnes DK, Madara JL. Neutrophil migration across model intestinal epithelia: monolayer disruption and subsequent events in epithelial repair. *Gastroenterology*. 1997; 113:1489–1500. [PubMed: 9352851]
32. Li Y, Brazzell J, Herrera A, Walcheck B. ADAM17 deficiency by mature neutrophils has differential effects on L-selectin shedding. *Blood*. 2006; 108:2275–2279. [PubMed: 16735599]
33. Hafezi-Moghadam A, Ley K. Relevance of L-selectin shedding for leukocyte rolling in vivo. *J Exp Med*. 1999; 189:939–948. [PubMed: 10075977]

34. Carson SD, Hobbs JT, Tracy SM, Chapman NM. Expression of the coxsackievirus and adenovirus receptor in cultured human umbilical vein endothelial cells: regulation in response to cell density. *J Virol.* 1999; 73:7077–7079. [PubMed: 10400813]
35. Vigi B, et al. Coxsackie- and adenovirus receptor (CAR) is expressed in lymphatic vessels in human skin and affects lymphatic endothelial cell function in vitro. *Experimental Cell Research.* 2009; 315:336–347. [PubMed: 19007771]
36. Excoffon KJDA, Hruska-Hageman A, Klotz M, Traver GL, Zabner J. A role for the PDZ-binding domain of the coxsackie B virus and adenovirus receptor (CAR) in cell adhesion and growth. *Journal of Cell Science.* 2004; 117:4401–4409. [PubMed: 15304526]
37. Leca G, Mansur SE, Bensussan A. Expression of VCAM-1 (CD106) by a subset of TCR gamma delta-bearing lymphocyte clones. Involvement of a metalloprotease in the specific hydrolytic release of the soluble isoform. *J Immunol.* 1995; 154:1069–1077. [PubMed: 7529789]
38. Severson EA, Parkos CA. Structural determinants of Junctional Adhesion Molecule A (JAMA) function and mechanisms of intracellular signaling. *Current Opinion in Cell Biology.* 2009; 21:701–707. [PubMed: 19608396]
39. Mandell KJ, Babbitt BA, Nusrat A, Parkos CA. Junctional adhesion molecule 1 regulates epithelial cell morphology through effects on beta 1 Integrins and Rap1 activity. *Journal of Biological Chemistry.* 2005; 280:11665–11674. [PubMed: 15677455]
40. Kirby I, et al. Adenovirus type 9 fiber knob binds to the coxsackie B virus-adenovirus receptor (CAR) with lower affinity than fiber knobs of other CAR-binding adenovirus serotypes. *Journal of Virology.* 2001; 75:7210–7214. [PubMed: 11435605]
41. Patzke C, et al. The coxsackievirus-adenovirus receptor reveals complex homophilic and heterophilic interactions on neural cells. *J Neurosci.* 2010; 30:2897–2910. [PubMed: 20181587]
42. van Raaij MJ, Chouin E, van der Zandt H, Bergelson JM, Cusack S. Dimeric structure of the coxsackievirus and adenovirus receptor D1 domain at 1.7 Å resolution. *Structure.* 2000; 8:1147–1155. [PubMed: 11080637]
43. Volk AP, et al. Priming of neutrophils and differentiated PLB-985 cells by pathophysiological concentrations of TNF-alpha is partially oxygen dependent. *J Innate Immun.* 2011; 3:298–314. [PubMed: 21088376]
44. Tucker KA, Lilly MB, Heck L Jr, Rado TA. Characterization of a new human diploid myeloid leukemia cell line (PLB-985) with granulocytic and monocytic differentiating capacity. *Blood.* 1987; 70:372–378. [PubMed: 3475136]
45. Parkos CA, Delp C, Arnaout MA, Madara JL. Neutrophil migration across a cultured intestinal epithelium. Dependence on a CD11b/CD18-mediated event and enhanced efficiency in physiological direction. *J Clin Invest.* 1991; 88:1605–1612. [PubMed: 1682344]
46. Balsam LB, Liang TW, Parkos CA. Functional mapping of CD11b/CD18 epitopes important in neutrophil-epithelial interactions: a central role of the I domain. *J Immunol.* 1998; 160:5058–5065. [PubMed: 9590256]
47. Denning TL, et al. Functional specializations of intestinal dendritic cell and macrophage subsets that control Th17 and regulatory T cell responses are dependent on the T cell/APC ratio, source of mouse strain, and regional localization. *J Immunol.* 2011; 187:733–747. [PubMed: 21666057]
48. Hopkins AM, et al. Epithelial cell spreading induced by hepatocyte growth factor influences paxillin protein synthesis and posttranslational modification. *Am J Physiol Gastrointest Liver Physiol.* 2004; 287:G886–898. [PubMed: 15191880]
49. Khounlotham M, et al. Compromised intestinal epithelial barrier induces adaptive immune compensation that protects from colitis. *Immunity.* 2012; 37:563–573. [PubMed: 22981539]

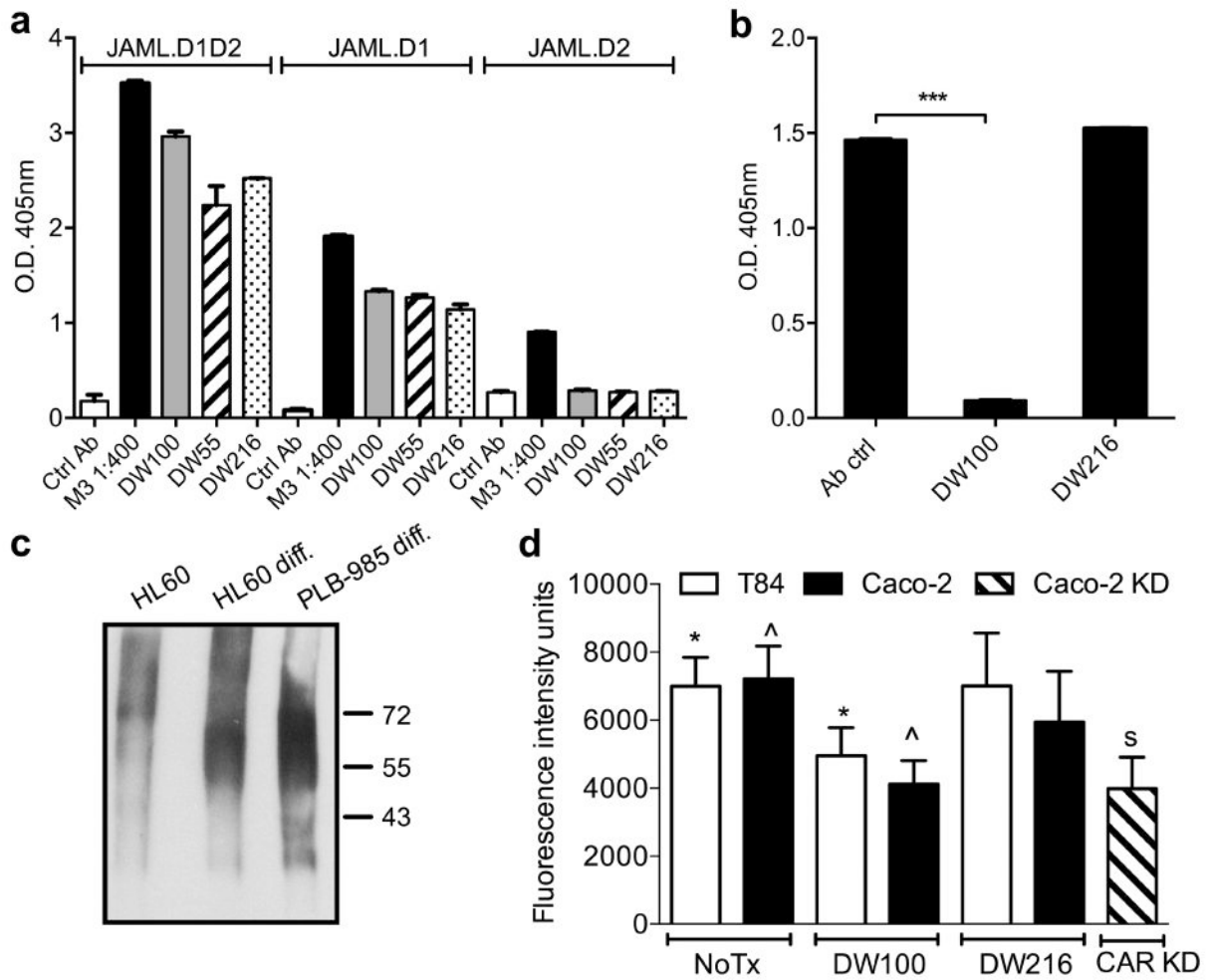


**Figure 1. Characterization of an anti-human JAML mAb that inhibits JAML-CAR binding**  
**(a)** Anti-JAML mAbs were added to Immulon plates coated with sJAML (JAML.D1D2), membrane distal (sJAML.D1) or membrane proximal (sJAML.D2) domains. Antibody binding was detected using goat anti-mouse HRP. M3 represents JAML antiserum collected from the sJAML-His immunized mouse before fusion. Anti-Myc mAb (9E10) was used as control. Both anti-JAML mAbs bound to the membrane distal domain (D1) of JAML. **(b)** mAbs to JAML (10  $\mu$ g/ml) were added to plates coated with sJAML followed by addition of CAR-GST (5  $\mu$ g/ml). CAR binding was detected by goat anti GST-HRP. DW100 inhibited CAR binding to sJAML, but DW216 had no effect. \*\*\*  $p < 0.01$  (significantly different). **(c)** JAML was immunoprecipitated from lysates of surface biotinylated cells, using DW216 mAb conjugated to sepharose beads. Western blot analysis using streptavidin-HRP revealed a broad protein band (55-70 kDa) in lysates from differentiated cells. **(d)** A functional role for JAML-CAR binding interactions was tested in cell adhesion assays. PMN ( $2.5 \times 10^5$ /well) labeled with CellTracker™ Green were allowed to adhere to T84 (white bars), Caco-2 (black bars) or to stable Caco-2 lacking CAR (CAR KD) monolayers, in the absence of extracellular  $Ca^{2+}$  (to open tight junctions and eliminate contributions to CD11b/CD18-mediated adhesion) without (NoTx) or in the presence of DW100 or DW216 (30  $\mu$ g/ml). DW100 but not DW216 reduced adhesion of PMN to epithelial monolayers to the same



levels observed after CAR knockdown. <sup>\*</sup>/<sup>^</sup> p<0.05 (significantly different from each other). <sup>S</sup> p<0.05 (significantly different from control). n=3 independent experiments.

Author Manuscript

Author Manuscript

Author Manuscript

Author Manuscript

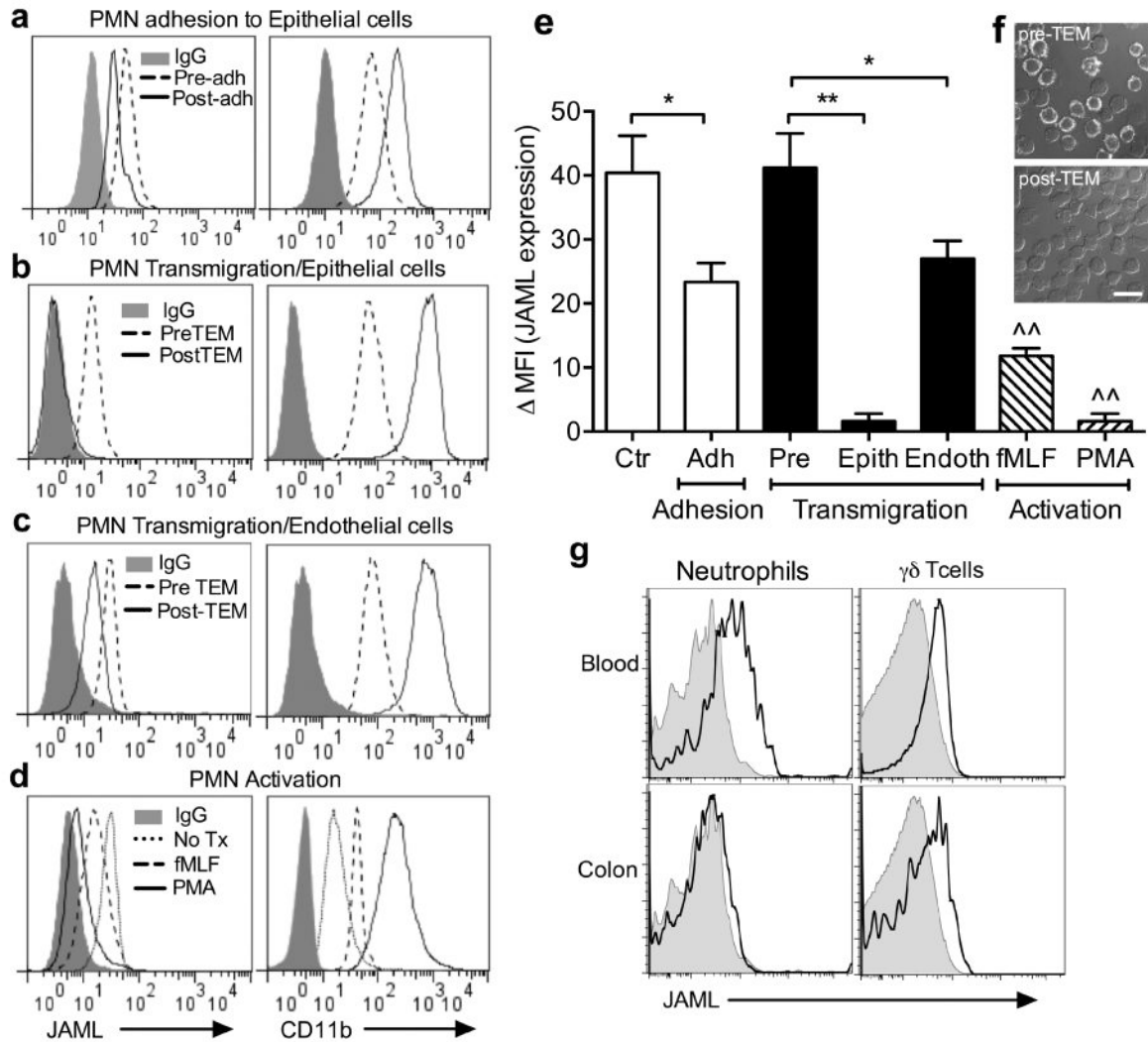


**Figure 2. JAML expression on PMN surface is lost during transmigration in-vitro and in-vivo** (a-f) JAML and CD18/CD11b (as an index of PMN activation) expression on human PMN was examined by flow cytometry. (a) JAML expression on PMN after adhesion to epithelial cells was quantified by staining with DW216 mAb (5 $\mu$ g/ml). PMN were distinguished from epithelial cells by gating on CD18/CD11b positive cells (CBRM 1/29, 5 $\mu$ g/ml). Adhesion to epithelium induced a partial loss of JAML. (b-c) PMN before or after migration across either T84 (b) or HDMVEC (c) monolayers were PFA-fixed and stained for JAML and CD11b/CD18 as described above. Complete loss of surface JAML was observed after transepithelial migration, but only partial loss after transendothelial migration. (d) JAML expression was examined after fMLF (100nM) and PMA (200nM) activation. fMLF activation resulted in partial loss of JAML, however stronger activation with PMA triggered complete loss of JAML. (e) Quantification of JAML expression, under the conditions specified above. \* p<0.05, \*\* p<0.01 \*\*\* p<0.001 (significantly different). ^^ p<0.01 (significantly different from control). n=4 independent experiments. (f) Representative immunofluorescence images of PMN before and after transepithelial migration. Scale bar is 10 $\mu$ m. (g) JAML expression (line histograms) was examined in-vivo, on murine circulating

(upper panels) and colonic lamina propria (bottom panels) PMN and  $\gamma\delta$ T-cells, and compared to that on B cells (do not express JAML, filled histograms). JAML expression was lost on PMN that infiltrated the colonic lamina propria, compared to circulating cells, but was unchanged on lamina propria  $\gamma\delta$ T-cells. The micrographs are representative of 3 independent experiments.

Author Manuscript

Author Manuscript

Author Manuscript

Author Manuscript

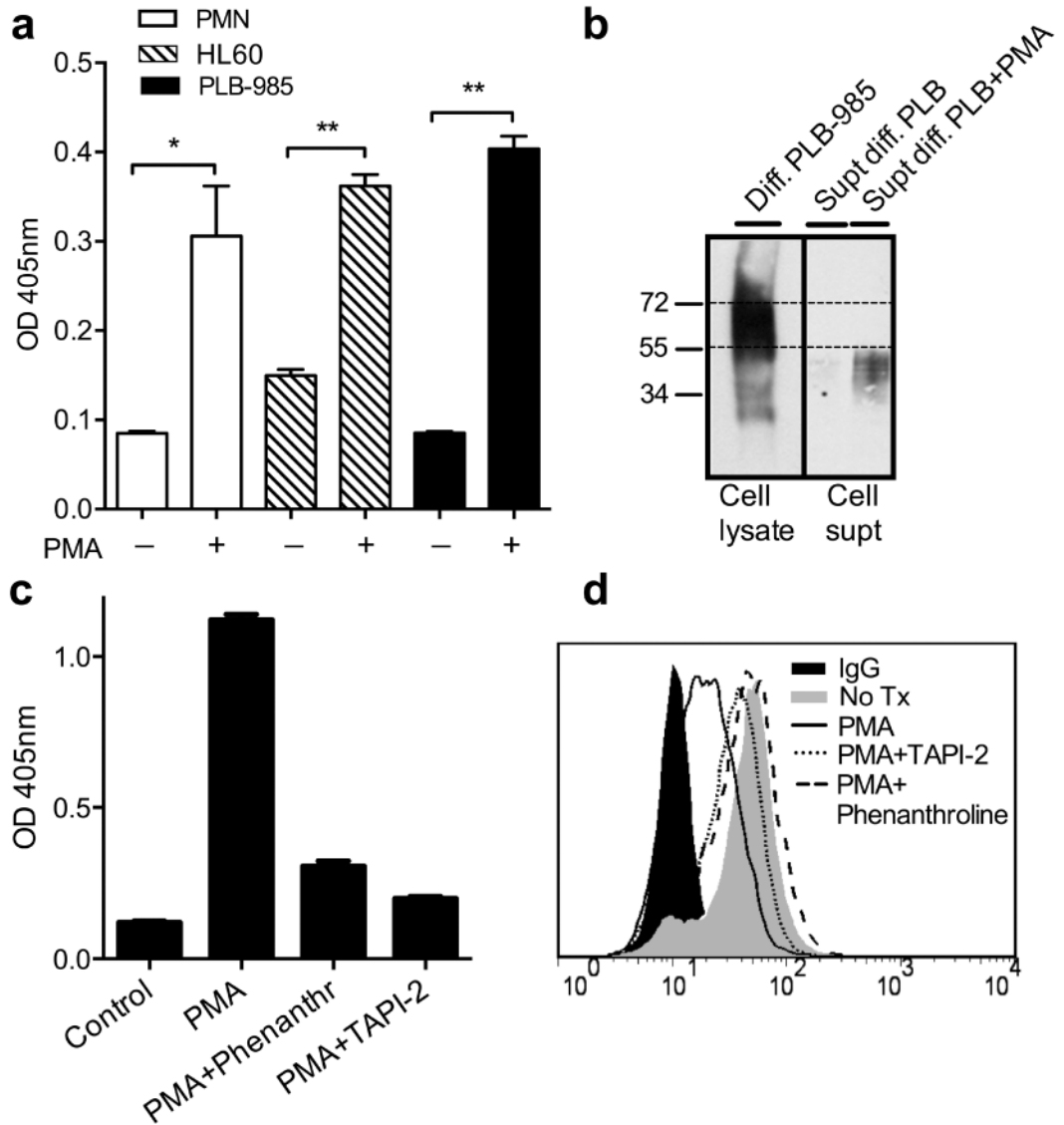


**Figure 3. JAML is cleaved from PMN surface by Zn<sup>++</sup>-dependent metalloproteases**  
**(a)** Supernatants of PMA activated (200nM) PMN ( $30 \times 10^6$  cells/condition), differentiated HL60 and PLB-985 cells, after removal of microparticles (ultra centrifugation,  $100K \times g$ , 30 minutes) were analyzed for the presence of shed JAML using a capture ELISA as described in Material and Methods. \*  $p < 0.05$ , \*\*\*  $p < 0.001$ , (significantly different).  $n = 4$  independent experiments. **(b)** JAML was immunoprecipitated using DW216-agarose bead conjugates from supernatants and total cell lysates of differentiated PLB-985 cells that were surface biotinylated and treated with or without PMA (200nM). JAML immunoprecipitated from stimulated cell supernatants appears as a wide protein band between  $\sim 45$ KD suggesting that it contains a majority of the extracellular domain of JAML. **(c)** Capture ELISA of JAML shedding from differentiated PLB-985 after PMA treatment in the presence or absence of Phenanthroline (5mM) and TAPI-2 (1 $\mu$ M), Zn<sup>++</sup> metalloprotease inhibitors. \*\*\*  $p < 0.001$ , (significantly different).  $n = 4$  independent experiments. **(d)** Inhibition of JAML shedding

from PLB-985 cells was confirmed by FACS analysis of cells stained with DW216. In the presence of inhibitors, PMA activation had no effect on JAML expression.

Author Manuscript

Author Manuscript

Author Manuscript

Author Manuscript

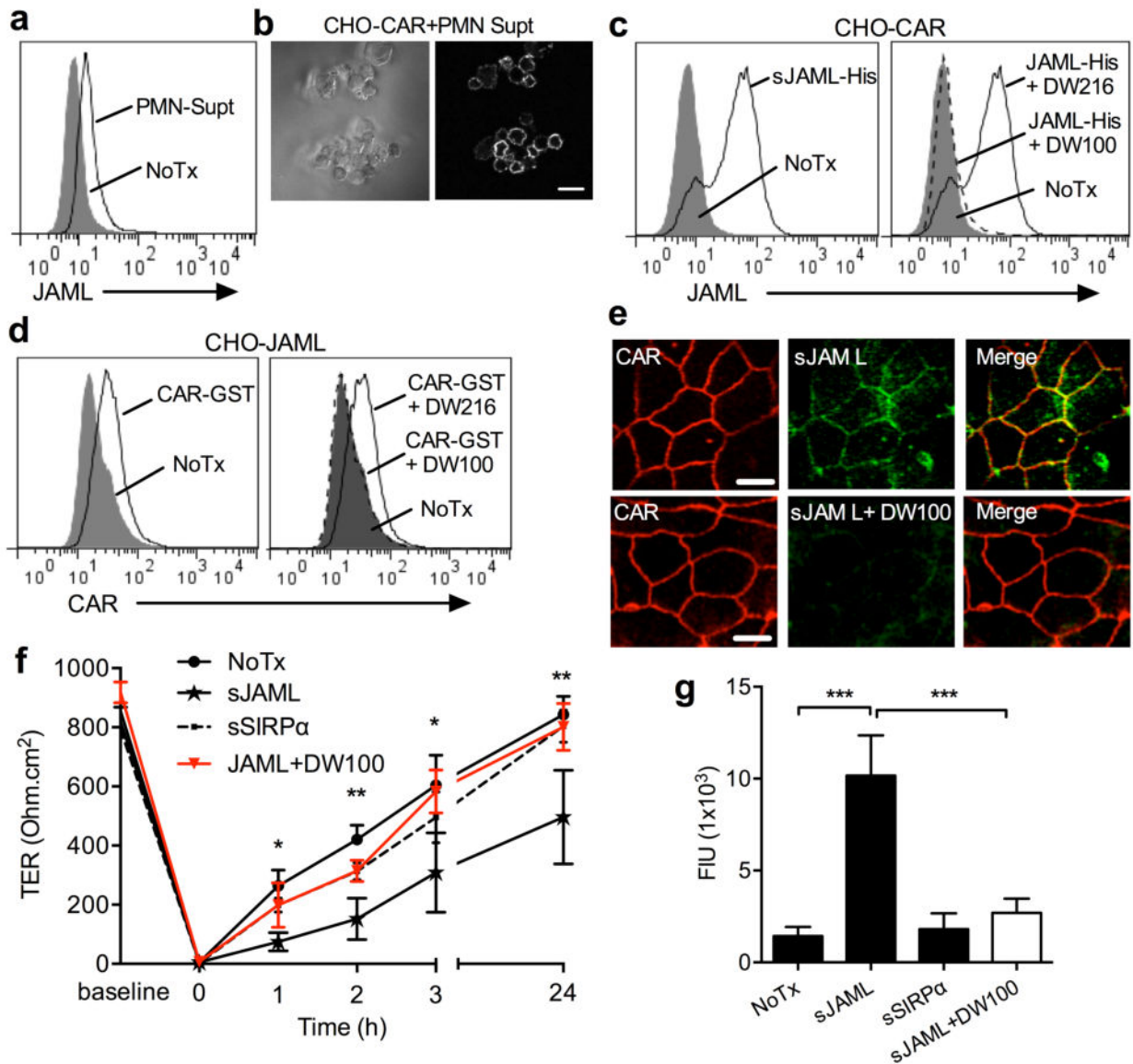


**Figure 4. Shed JAML binds to CAR and inhibits epithelial barrier function**

(a-b) CHO-CAR stable transfectants were incubated with supernatants from PMA activated PMN ( $30 \times 10^6$ /condition, 1h on ice), and JAML binding to CAR was examined by flow cytometry (a) and confocal immunofluorescence microscopy (b). Scale bar is  $20 \mu\text{m}$ . (c) CHO-CAR stable transfectants were incubated with soluble JAML-His alone (sJAML,  $20 \mu\text{g/ml}$ ) or in the presence of DW216 or DW100 mAbs ( $30 \mu\text{g/ml}$ , right panel). JAML binding to CAR was measured by flow cytometry and compared to untreated CHO-CAR (NoTx). (d) CHO-JAML stable transfectants were incubated with CAR-GST alone ( $20 \mu\text{g/ml}$ , left panel) or in the presence of DW216 or DW100 mAbs ( $30 \mu\text{g/ml}$ , right panel) and binding was measured by flow cytometry. DW100 but not DW216 prevented JAML-CAR interactions in CHO cells. Flow micrographs are representative of 4 independent experiments. (e) Representative immunofluorescence images confirm binding of sJAML to epithelial CAR. T84 monolayers, that were transiently preincubated in  $\text{Ca}^{2+}$  free buffer to

increase access to TJs, were incubated with sJAML (20 $\mu$ g/ml) with/without DW100 mAb (30 $\mu$ g/ml) and stained for JAML (DW216, 10 $\mu$ g/ml) and CAR (H-300, 10 $\mu$ g/ml). Colocalization of JAML and CAR is evident. Scale bar is 20 $\mu$ m. **(f)** Barrier formation of T84 monolayers after a calcium switch assay was determined by TER measurements without (NoTx), or in the presence of control protein sSIRP $\alpha$  or sJAML (20 $\mu$ g/ml) with/without DW100 mAb (30 $\mu$ g/ml) at time points as indicated. \*  $p < 0.05$ , \*\*  $p < 0.005$  (significantly different from sJAML group).  $n = 4$  independent experiments. **(g)** Flux of FITC-dextran (3Kd) was measured after 24h in a parallel experiment identical to that in panel D. Addition of soluble JAML but not SIRP $\alpha$  inhibits epithelial barrier recovery. The deleterious effects of sJAML on epithelial permeability were reversed with DW100 mAb. FIU, fluorescence intensity units. \*\*\*  $p < 0.001$  (significantly different).  $n = 4$  independent experiments.

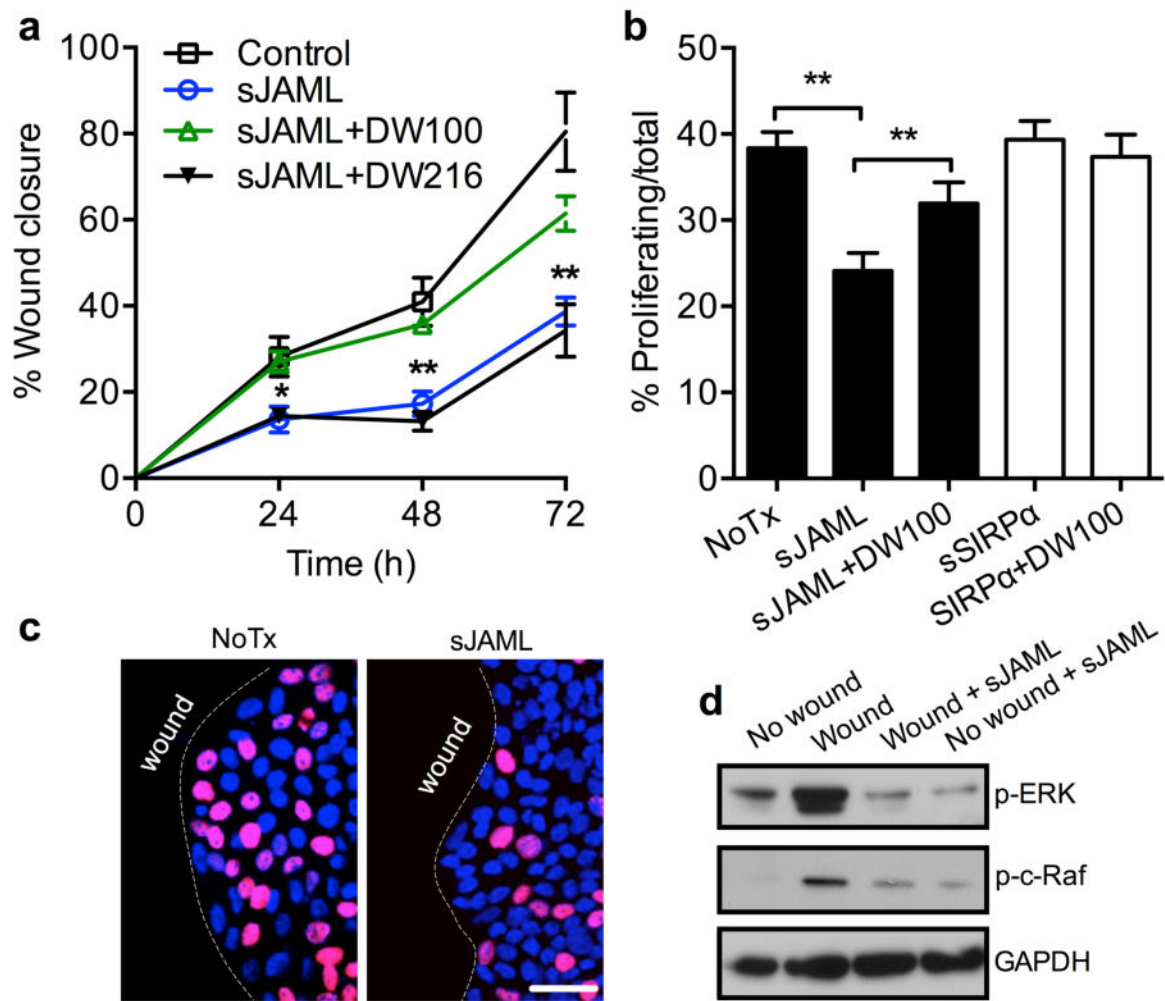


**Figure 5. Ligand of CAR by sJAML inhibits wound closure and decreases epithelial cell proliferation**

(a) Intestinal epithelial monolayers grown to confluence were wounded by introduction of single linear scratch wounds. Wound closure was monitored over 72h in the absence or presence of sJAML (20 $\mu$ g/ml) and DW100 (JAML neutralizing antibody, 50 $\mu$ g/ml). Addition of sJAML significantly inhibited wound closure. Importantly, in the presence of DW100, but not DW216, the inhibition was reversed. \* $p < 0.05$ , \*\*  $p < 0.005$  (significantly different from sJAML group).  $n = 4$  independent experiments. (b) Epithelial monolayers were wounded as described above and cell proliferation at the wound edge was assessed by EdU incorporation assay after 24 hours in the presence of either sJAML or sSIRP $\alpha$  (30 $\mu$ g/ml), with or without addition of DW100 mAb. Data are presented as percentage of proliferating cells (positively stained with EdU) relative to total cells per field. \*\*  $p < 0.01$  (significantly different). Cells were counted in 7 randomly selected fields in 4 independent experiments. (c) Representative images depicting the decrease in proliferating cells at the wound edge in the presence of JAML. The scale bar is 50 $\mu$ m. (d) sJAML inhibits wound closure by signaling through the ERK pathway. Western blots from lysates of wounded T84



monolayers demonstrating decreased p-ERK and p-C-Raf signaling after addition of sJAML compared to untreated monolayers.

Author Manuscript

Author Manuscript

Author Manuscript

Author Manuscript

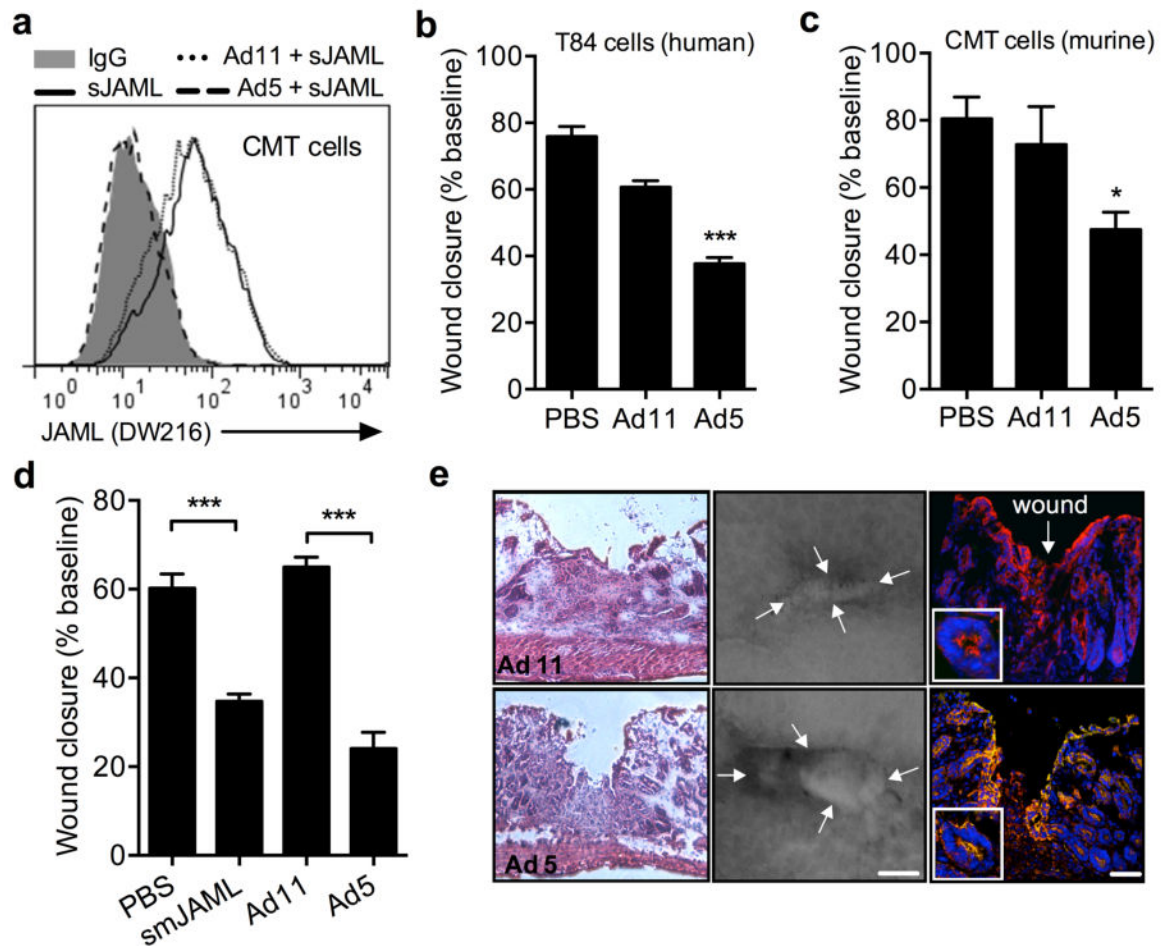


**Figure 6. CAR ligation by Ad5 or sJAML inhibits epithelial wound repair in-vitro and in-vivo** (a) CAR expressing murine epithelial cells (CMT) were incubated with sJAML (20μg/ml) in the presence of Ad5 (10μg/ml) or Ad11 (10μg/ml). Addition of Ad5, but not Ad11 prevented JAML binding. n=4 independent experiments. (b-c) Scratch wound assays were performed to examine the effects of CAR ligation by Ad5 (10μg/ml) and Ad11 (10μg/ml) on wound closure of T84 (human) and CMT epithelial cells. Addition of Ad5 but not Ad11 significantly decreased wound closure in both cell types. The data show quantification of wound area 72h post-wounding. \* p<0.05, \*\*\* p<0.001 (significantly different from PBS). n=4. (d-e) In-vivo examination of the effects of CAR ligation by Ad5, Ad11 and murine sJAML on mucosal wound healing, using colonoscopic biopsy techniques. (d) Administration of sJAML (20μg/100 l, I.P. twice daily) and Ad5 but not Ad11 (10μg/100μl, I.P. twice daily) or PBS significantly delayed wound closure. The data show quantification of wound areas 4 days post-wounding \*\*\* p<0.005 (double blinded study, 5 mice/group). n=3 independent experiments. (e) Hematoxylin/eosin stained wounds sections (left panels) and representative images of excised whole mounts of mucosal wounds (middle panels, the bar is 200μm) at day 4 post-wounding demonstrate near complete healing in the presence of Ad11 (upper panels) but not Ad5 (bottom panels). Ad5 colocalization (yellow) with CAR in wounded regions was confirmed by immunofluorescence staining (CAR, red and His tagged Ad5 and Ad11, green).

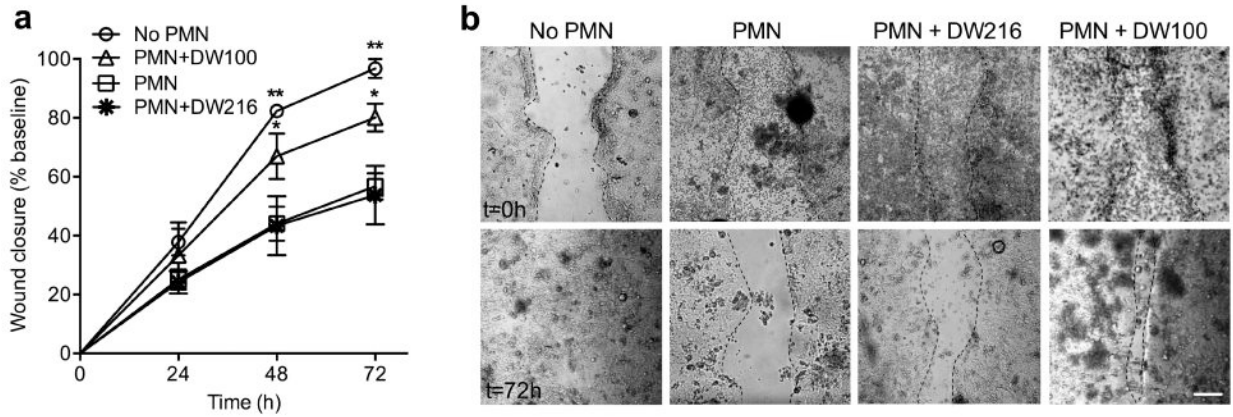


**Figure 7. Inhibitory effects of PMN on epithelial wound repair are significantly attenuated by blocking CAR-JAML interactions**

(a) T84 monolayers grown to confluence were wounded by introduction of single linear scratch wounds. Wound closure was monitored over 72 h in the absence or presence of PMN ( $1 \times 10^6$ /well), and/or DW100 (JAML neutralizing antibody,  $30 \mu\text{g/ml}$ ) and DW216 ( $30 \mu\text{g/ml}$ ) antibodies. The presence of PMN significantly inhibited wound closure. Importantly, addition of DW100 but not DW216 significantly reversed PMN-mediated inhibition of wound closure. \*  $p < 0.05$ , \*\*  $p < 0.005$  (significantly different from PMN group).  $n = 4$  independent experiments. (b) Representative images of epithelial monolayers immediately after wounding and addition of PMN ( $t = 0$ , upper panels), and after 72 hours ( $t = 72$ h, bottom panels) demonstrating inhibitory effects of PMN on wound healing, and reversal of inhibition with DW100 mAb. The scale bar is  $25 \mu\text{m}$ .

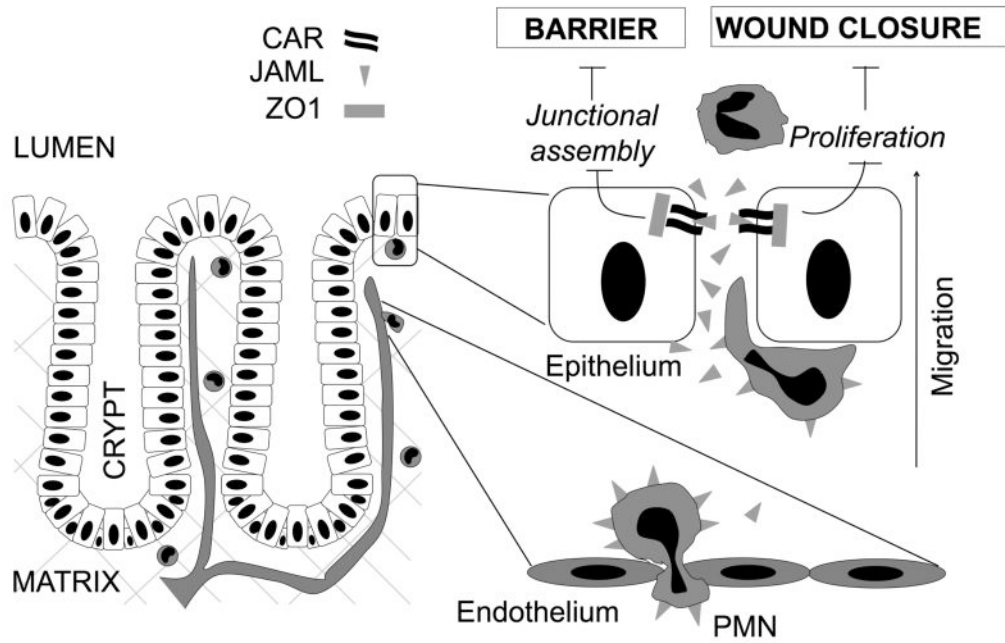


**Figure 8. Model depicting a paracrine role of JAML in inhibition of intestinal epithelial restitution during acute inflammation**

Acute PMN recruitment to mucosal surfaces in response to microbes or injury occurs in several steps. First PMN exit the microcirculation by migrating across the vascular endothelium where JAML is mostly retained on the PMN cell surface. As PMN migrate across the epithelium, JAML is cleaved from the cell surface where it binds to CAR at tight junctions. Soluble JAML binding to CAR results in disruption of CAR-mediated signaling events and inhibits tight junction reassembly/barrier formation secondary to PMN transmigration. Furthermore, soluble JAML inhibits CAR-dependent epithelial proliferation at wounds in close proximity to migrating/activated PMN resulting in delayed mucosal healing. Thus, release of JAML would provide an efficient pro-inflammatory mechanism to facilitate recruitment of additional leukocytes and thus aid in clearance of invading microorganisms. However, sustained release of JAML under pathologic conditions associated with persistence of large numbers of infiltrated PMN would inhibit mucosal healing.